Inorganic Chemistry

Article

pubs.acs.org/IC

Non-Innocence of 1,4-Dicyanamidobenzene Bridging Ligands in Dinuclear Ruthenium Complexes.

Mohommad M. R. Choudhuri,[†] Wolfgang Kaim,[‡] Biprajit Sarkar,[§] and Robert J. Crutchley*[,†]

[†]Chemistry Department, Carleton University, Ottawa, Ontario K1S 5B6, Canada

[‡]Institut für Anorganische Chemie, Universität Stuttgart, Pfaffenwaldring 55, DE 70550 Stuttgart, Germany

[§]Inorganic Chemistry, Freie Universitat Berlin, Fabeckstrasse 34-36, DE 14195 Berlin, Germany

Supporting Information

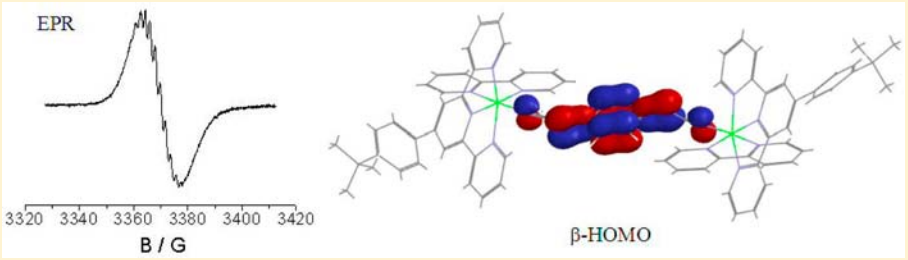

ABSTRACT: Four dinuclear complexes, $[\{Ru^{II}(ttpy)(bpy)\}_2(\mu\text{-L})][PF_6]_2$, where bpy is 2,2′-bipyridine, ttpy is 4-(*tert*-butylphenyl)-2,2′:6′,2″-terpyridine, and L is 2,5-dimethyl-, 2,5-dichloro-, 2,3,4,5-tetrachloro- and unsubstituted 1,4-dicyanamidebenzene dianion have been synthesized and characterized. Electron paramagnetic resonance (EPR) spectroscopy of electrogenerated $[\{Ru(ttpy)(bpy)\}_2(\mu\text{-L})]^{3+}$ ions shows largely ligand centered spin and thus the complexes' oxidation states are best formulated as $[Ru(II), L^{\bullet-}, Ru(II)]^{3+}$. Visible-NIR and IR spectra of $[\{Ru(ttpy)(bpy)\}_2(\mu\text{-L})]^{3+,4+}$ ions were also obtained by spectroelectrochemical methods. For the $[\{Ru(ttpy)(bpy)\}_2(\mu\text{-L})]^{3+}$ ions, the significant variations in the spectra were rationalized in terms of an increased ruthenium contribution to the singly occupied molecular orbital with increasing number of chloro substituents on the bridging ligand L.

INTRODUCTION

Interest in non-innocent (redox-active) ligands stems not only from examples in bioinorganic chemistry[1] but also with respect to catalysis[2] and the design of electro-optic materials.[3] For the latter, there are many examples of mixed-valence complexes whose properties (electrochemistry, dipole moment, NIR absorption) are determined by the degree of noninnocence of a bridging ligand.[4] Purposeful design of donor−acceptor systems and materials require that the expression and recognition of these properties be understood. Research into the complexes of the redox active 1,4-dicyanamidebenzene dianion ($dicyd^{2-}$) bridging ligand is illustrative.

$[\{Ru(NH_3)_5\}_2(\mu\text{-dicyd})]^{3+,4+,5+}$ ions have been shown[5] by electron paramagnetic resonance (EPR) and ^1H NMR evidence to involve a singly occupied molecular orbital (SOMO) of mostly metal character with the bridging ligand remaining $dicyd^{2-}$. Density functional theory (DFT) calculations of $[\{Ru(NH_3)_5\}_2(\mu\text{-dicyd})]^{3+}$ in the gas phase gave a mostly ligand-based SOMO, in disagreement with experiment, and could only be reconciled with the EPR and NMR data by invoking a strong donor−acceptor interaction between solvent molecules and the ammine protons and cyanamide groups. In contrast, Bonvoisin et al.[6] provided EPR and crystallographic evidence that the complex $[\{Ru(trpy)(thd)\}_2(\mu\text{-dicyd})]^+$, where trpy is 2,2′;6′,2″-terpyridine and thd^- is the 2,2,6,6-tetramethyl-3,5-heptanedionate anion, possesses two Ru(II) ions bridged by a radical $dicyd^-$ ligand. Why does replacing the ammines with trpy and thd cause the destabilizing of $dicyd^{2-}$ relative to Ru(II)? Clearly, the solvent donor−acceptor interaction for $[\{Ru(trpy)(thd)\}_2(\mu\text{-dicyd})]^+$ is not as great compared to dinuclear ammine complexes, and Ru(II) is stabilized by the trpy and thd^- coordination sphere. This stabilization should be even greater if thd^- is replaced by the neutral acceptor 2,2′-bipyridine (bpy), and it is thus likely that the previously reported $[\{Ru(trpy)(bpy)\}_2(\mu\text{-dicyd})]^{3+}$ also possesses a mostly ligand-localized SOMO.[7] The highest occupied molecular orbital (HOMO) of the $dicyd^{2-}$ bridging ligand can be significantly perturbed by electron donating or withdrawing substituents and this creates an opportunity to study a perturbed, mostly ligand-localized SOMO by spectroscopic methods.

For this study, four dinuclear complexes, $[\{Ru(ttpy)(bpy)\}_2(\mu\text{-L})][PF_6]_2$, where ttpy is 4-(*tert*-butylphenyl)-2,2′:6′,2″-terpyridine and L is 2,5-dimethyl-, 2,5-dichloro-, 2,3,4,5-tetrachloro- and unsubstituted 1,4-dicyanamidebenzene dianion have been synthesized and characterized. EPR spectroscopy was used to establish unambiguously the

Received: May 26, 2013
Published: September 20, 2013

dx.doi.org/10.1021/ic401316g | *Inorg. Chem.* 2013, 52, 11060−11066

oxidation states of the $[\{Ru(ttpy)(bpy)\}_2(\mu\text{-L})]^{3+}$ complexes and the complexes' visible-NIR and IR spectra were derived by spectroelectrochemical methods. The spectral variation that is observed can be related to an increase in metal character of the SOMO with electron-withdrawing substituents on the dicyd^{2-} bridging ligand.

EXPERIMENTAL SECTION

Reagents. The organic solvents used for spectroscopy and electrochemistry were distilled under reduced pressure and stored under argon. All solvents were dried with an appropriate reagent. Acetonitrile (HPLC grade, Aldrich) was distilled in the presence of phosphorus pentoxide. *N*,*N*′-dimethylformamide (DMF) and propylene carbonate were dried overnight and distilled in the presence of aluminum oxide (neutral grade) which had been previously activated by heating to 300 °C for 3 h. The mononuclear complex, $[Ru(trpy)(bpy)(2,4\text{-}Cl_2pcyd)][PF_6]$, where trpy is 2,2′;6′,2″-terpyridine, bpy is 2,2′-bipyridine, and 2,4-Cl_2pcyd$^-$ is 2,4-dichlorophenylcyanamide has been previously prepared.[8] $TlNO_3$ (BDH) (***Caution!**: highly toxic*) and 2,2′-bipyridine (Aldrich) were used as received. 1,4-Dicyanamidebenzene ($dicydH_2$) and its derivatives 2,5-dimethyl-($Me_2dicydH_2$), 2,5-dichloro- ($Cl_2dicydH_2$), and 2,3,5,6-tetrachloro-1,4-dicyanamidobenzene ($Cl_4dicydH_2$) were prepared by literature methods.[9] Both $Cl_2dicydH_2$ and $Cl_4dicydH_2$ possessed a significant impurity of the guanidine dimer as shown by a strong IR υ(C═N) band at approximately 1680 cm^{-1}. This dimer impurity reverts to a monomer in basic solutions and does not affect the isolation of the thallium salt of the ligand as discussed previously.[10] Thallium salts (***Caution**: highly toxic*) of dicyd^{2-} and its substituted derivatives were prepared by using the general method described below for $Tl_2[Me_2dicyd]$) and were used without further purification. These salts are only slightly soluble in strong donor solvents, but this is sufficient for the reactions described below.

Preparation of Thallium 2,5-Dimethyl-1,4-dicyanamidebenzene Dianion, $Tl_2[Me_2dicyd]$. $Me_2dicydH_2$ (0.4 g) was dissolved in 100 mL of gently boiling 3:1 acetone:water and then filtered. Approximately 1.5 mL of triethylammine was added to the filtrate, followed quickly by a warm solution of 1.3 g of $TlNO_3$ in 25 mL of water. The slightly blue solution was gently boiled for 5 min forming a yellow precipitate which was filtered and washed with acetone and water and finally acetone and allowed to dry. Yield: 0.7 g (54%). Anal. Calcd for $C_{10}H_8N_4Tl_2$: C, 20.26; H, 1.36; N, 9.45. Found: C, 20.17; H, 1.16; N, 9.43. ^{1}H NMR (DMSO-d_6): the poor solubility and oxidation to the radical by trace oxygen made the Me_2dicyd^{2-} chemical shift assignment unreliable.

Preparation of Thallium 1,4-Dicyanamidebenzene Dianion, $Tl_2[dicyd]$. Prepared in the same manner as $Tl_2[Me_2dicyd]$. Yield: 77%). Anal. Calcd for $C_8H_4N_4Tl_2$: C, 17.01; H, 0.71; N, 9.92. Found: C, 17.18; H, 0.58; N, 9.75. ^{1}H NMR (DMSO-d_6): 6.32 (4H, s) ppm.

Preparation of Thallium 2,5-Dichloro-1,4-dicyanamidebenzene Dianion, $Tl_2[Cl_2dicyd]$. Prepared in the same manner as $Tl_2[Me_2dicyd]$. Yield: 60%. Anal. Calcd for $C_8H_4N_4Cl_2Tl_2$: C, 15.16; H, 0.32; N, 8.84. Found: C, 15.19; H, 0.33; N, 8.75. ^{1}H NMR (DMSO-d_6): 6.73 (2H, s) ppm.

Preparation of Thallium 2,3,5,6-Tetrachloro-1,4-dicyanamidebenzene Dianion, $Tl_2[Cl_4dicyd]\cdot 0.25[HN(CH_2CH_3)_3][NO_3]$. Prepared in the same manner as $Tl_2[Me_2dicyd]$. Yield: 48%. Anal. Calcd for $C_{9.5}H_4N_{4.5}Cl_4\ O_{0.75}Tl_2$: C, 15.34; H, 0.54; N, 8.47. Found: C, 15.43; H, 0.3; N, 8.66. This procedure was repeated twice, and the elemental analyses gave the same triethylammonium impurity whose presence was confirmed by ^{1}H NMR.

Preparation of 4-(*tert*-Butylphenyl)-2,2′:6′,2″-terpyridine (ttpy). This compound has been prepared previously[11] but the method described below eliminates the need to isolate the penta-1,5-dione derivative. 4-*tert*-Butylbenzaldehyde (5 g) and 2-acetylpyridine (13 g) were added to 800 mL of methanol in a 2 L Erlenmeyer flask. To the stirred solution were added 330 mL of concentrated aqueous ammonia and 65 mL of 3.75 M NaOH. The Erlenmeyer flask was covered with a watch glass, and the reaction solution allowed to stir for 4 days during which time the solution became yellow and then cloudy with the precipitation of the product. The reaction mixture was filtered and the light-green product washed with copious water and allowed to air-dry. Recrystallization from acetone/water (4:1) yielded 3.0 g, (26%), of light-green flaky crystals, mpt. 194−195 °C. Anal. Calcd for $C_{25}H_{23}N_3$: C, 82.16; H, 6.34; N, 11.50. Found: C, 82.13; H, 6.43; N, 11.57. ^{1}H NMR ($CDCl_3$): 1.38 (9H, s), 7.33 (2H, dd), 7.52 (2H, d), 7.85 (2H, dd), 7.86 (2H, d), 8.66 (2H, d), 8.72 (2H, d), 8.75 (2H, s), in agreement with literature.[11]

Preparation of $Ru(ttpy)Cl_3\cdot H_2O$. A mixture of $RuCl_3\cdot 3H_2O$ (2.4 g) and ttpy (3.2 g) in absolute ethanol (600 mL) was refluxed 14 h. The dark-brown reaction mixture was cooled and then filtered. The dark-brown product was washed with water, followed by absolute ethanol and then diethylether and vacuum-dried. Yield: 4.2 g, 78%. Anal. Calcd for $C_{25}H_{25}N_3OCl_3Ru$: C, 50.81; H, 4.26; N, 7.11. Found: C, 50.53; H, 3.83; N, 6.94.

Preparation of $[Ru(ttpy)(bpy)Cl][PF_6]$. $Ru(ttpy)Cl_3\cdot H_2O$ (2 g) and 2,2′-bipyridine (0.52 g) were added to 400 mL of water/ethanol (2:1) and refluxed under argon for 14 h. The reaction solution was allowed to cool slightly before adding LiCl (2 g) and refluxing for a further 1 h. The reaction solution was filtered and to the hot filtrate was added 4 g of NH_4PF_6, precipitating the desired product which was immediately filtered off, washed with water, and allowed to air-dry. Recrystallization by diffusing ether into an acetone solution of the complex yielded dark brown crystals. Yield 2.0 g (74%). Anal. Calcd for $C_{35}H_{31}N_5ClPF_6Ru$: C, 52.34; H, 3.89; N, 8.72. Found: C, 52.16; H, 3.78; N, 8.71. ^{1}H NMR (DMSO-d_6): 10.12 (d, 2H), 9.16 (s, 4H), 8.92 (d, 6H), 8.65 (d, 2H), 8.37 (t, 2H), 8.24 (d, 4H), 8.10−8.00 (m, 6H), 7.79 (t, 2H), 7.72 (d, 4H), 7.64 (d, 4H), 7.44−7.37 (m, 6H), 7.12 (t, 2H), 1.42 (s, 18H). Filtering off the complex from the hot solution keeps most impurities in solution and yields an almost pure reagent complex.

Complex Synthesis. The complexes of Cl_2dicyd^{2-} and Cl_4dicyd^{2-} could be purified by chromatography by using alumina (Grade III) and eluting with DMF. However, under the same conditions, the complexes of dicyd^{2-} and Me_2dicyd^{2-} proved to be air sensitive. For the latter complexes, fractional crystallization under an argon atmosphere yielded pure product in good yield.

Preparation of $[\{Ru(ttpy)(bpy)\}_2(\mu\text{-}Me_2dicyd)][PF_6]_2$ 1. $[Ru(ttpy)(bpy)Cl][PF_6]$ (1.0 g) and $Tl_2[Me_2dicyd]$ (0.3 g) were placed in 175 mL of DMF and refluxed under argon for 40 h during which time the reaction solution changed color from violet-purple to a brownish-purple and TlCl precipitated. The reaction mixture was gravity filtered through Celite, and the filtrate's volume reduced to 5−10 mL. The crude complex was precipitated by the addition of ether (300 mL), filtered, and allowed to air-dry. Crude yield: 0.8 g. Separation of the dinuclear complex from monomer impurity was achieved under an argon atmosphere by dissolving the complex in 20 mL of CH_3CN, filtering, and to the filtrate slowly adding approximately 40 mL of toluene. The precipitated dinuclear complex was filtered, washed with toluene and then ether, and vacuum-dried. Yield: 0.35 g, 33% Anal. Calcd for $C_{80}H_{70}N_{14}P_2F_{12}Ru_2$: C, 55.88; H, 4.10; N, 11.40. Found: C, 55.39; H, 4.36; N, 11.75. IR (KBr), ν(NCN) = 2104 cm^{-1}.

Preparation of $[\{Ru(ttpy)(bpy)\}_2(\mu\text{-dicyd})][PF_6]_2\cdot 1.6(toluene)\cdot 4H_2O$ 2. This was prepared as for **1** but precipitated with toluene and water of crystallization as shown by ^{1}H NMR. Yield: 0.30 g, 31%. Anal. Calcd for $C_{89.2}H_{86.8}N_{14}O_4P_2F_{12}Ru_2$: C, 56.06; H, 4.58; N, 10.26. Found: C, 56.11; H, 4.19; N, 10.50. IR (KBr), ν(NCN) = 2156 cm^{-1}.

Preparation of $[\{Ru(ttpy)(bpy)\}_2(\mu\text{-}Cl_2dicyd)][PF_6]_2$ 3. $[Ru(ttpy)(bpy)Cl][PF_6]$ (1 g) and $Tl_2[Cl_2dicyd]$ (0.4 g) were placed in 175 mL of DMF and refluxed under argon for 60 h during which time the reaction solution changed color from violet-purple to a brownish-purple and TlCl precipitated. The reaction mixture was gravity filtered through Celite and the filtrate's volume reduced to 50 mL. The crude complex was precipitated by the addition of ether (300 mL), filtered, and allowed to air-dry. Crude yield: 0.7 g. Chromatography using alumina (Type III) and elution with CH_3CN:toluene 1:1 yielded an orange band, followed by a purple reagent band and finally a brown band. The latter was collected and the acetonitrile evaporated off yielding the desired product suspended in toluene. Yield 0.23 g (21%).

dx.doi.org/10.1021/ic401316g | *Inorg. Chem.* 2013, 52, 11060−11066

Anal. Calcd for $C_{78}H_{64}N_{14}Cl_2P_2F_{12}Ru_2$: C, 53.22; H, 3.66; N, 11.14. Found: C, 53.36; H, 3.43; N, 11.46. IR (KBr), ν(NCN) = 2141 cm^{-1}.

Preparation of [{Ru(ttpy)(bpy)}$_2$(μ-Cl$_4$dicyd)][PF$_6$]$_2$·0.5toluene·CH$_3$CN 4. This was prepared in the same manner as **3**. Recrystallized from CH_3CN/toluene. Yield 15%. Anal. Calcd for $C_{83.5}H_{69}N_{15}Cl_4P_2F_{12}Ru_2$: C, 52.33; H, 3.63; N, 10.96. Found: C, 52.08; H, 3.54; N, 11.10. IR (KBr), ν(NCN) = 2156 cm^{-1}.

Physical Measurements. *Electrochemistry.* Cyclic voltammetry studies were performed using a Metrohm Autolab potentiostat/galvanostat PGSTAT30. DMF (Sigma-Aldrich, ChromosolvPlus, 99.9%, HPLC grade) was used for the studies. A three electrode arrangement consisting of a platinum disk electrode working electrode (BAS 1.6 mm diameter), a platinum wire auxiliary electrode, and a silver-wire quasi-reference electrode was used. The electrochemical cell consisted of a double jacketed glass container with an internal volume of 15 mL. Ferrocene ($E°$= 0.665 V versus NHE)[12] was used as internal reference, and TBAH (0.1M) was the supporting electrolyte. Argon gas was bubbled into the solutions for 10−15 min to degas them before scans were recorded. An optically transparent thin-layer electrochemical (OTTLE) cell was used to conduct spectroelectrochemical studies.[7,13−15] ITO (indium−tin oxide) coated glass served as working and counter electrodes and AgCl/Ag was used as reference electrode. The solvents and supporting electrolyte were the same as those used for cyclic voltammetry. Potential was varied between 0.00 and 1.10 V during the experiment, and spectra were collected on a UV−vis-NIR Cary 5 spectrophotometer.

NMR Studies. ^{1}H NMR spectra were obtained at ambient temperature by using Bruker AMX-400 NMR or Bruker 300 Ultra Shield spectrometers and referenced to TMS (0.00 ppm)

EPR Spectroscopy. EPR spectra of the complexes were recorded in DMF at room temperature to 4 K by using a Bruker system EMX, and a continuous flow cryostat ESR 900 of Oxford Instruments was used for this purpose.

Semi-Empirical Calculations. PM3 calculations of orbital energies and display of wave functions were obtained with Spartan V.10 software.

RESULTS AND DISCUSSSION

The complexes **1**−**4** were prepared by metathesis in refluxing DMF as shown in Scheme 1. The precipitation of TlCl removes chloride from the reaction solution and ensures a reasonable yield of complex. Unfortunately, the purification of **1** and **2** proved problematic because of their tendency to oxidize during chromatography on alumina. This was solved by the fortuitous discovery that the dinuclear complexes were far less soluble in acetonitrile/toluene solvent mixtures as compared to mononuclear complexes and could therefore be preferentially precipitated by the addition of toluene to an acetonitrile solution of the crude product. The ^{1}H NMR spectra of **1**−**4** (Supporting Information, Figures S1−S4) and elemental analyses were consistent with their formulation. Assignments of the ttpy chemical shifts were determined using COESY analysis (Supporting Information, Figures S5−S8 and Table S1).

Scheme 1

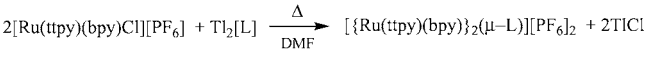

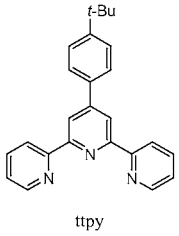

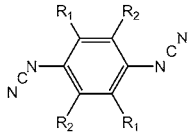

Complex	L	R_1	R_2
1	Me_2dicyd^{2-}	H	CH_3
2	$dicyd^{2-}$	H	H
3	Cl_2dicyd^{2-}	H	Cl
4	Cl_4dicyd^{2-}	Cl	Cl

Figure 1 shows the cyclic voltammograms of the [{Ru(ttpy)(bpy)}$_2$(μ-L)](PF$_6$)$_2$ compounds, and Table 1 summarizes the electrochemical data. Two oxidation couples are observed ranging from −0.3 to 1.4 V versus NHE in DMF. For each couple, the anodic and cathodic waves are of equal current but with peak to peak separation greater than 58 mV. The latter occurs when heterogeneous electron transfer is slow and identifies these one-electron oxidations as quasi-reversible

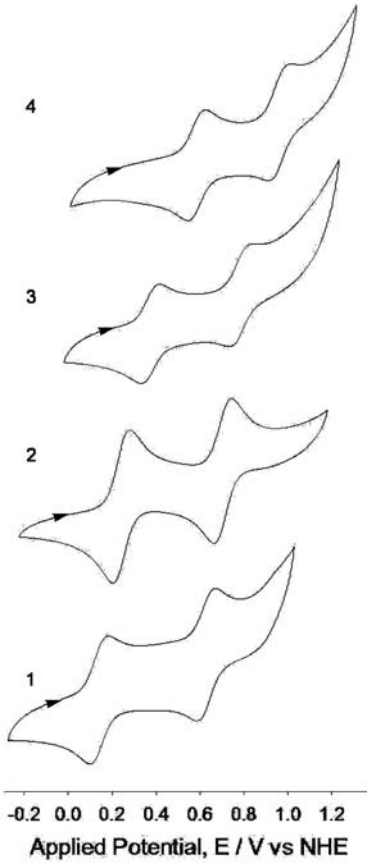

Figure 1. Cyclic voltammetry of [{Ru(ttpy)(bpy)}$_2$(μ-L)]$^{2+}$ in DMF, 0.1 M TBAH; L = Me_2dicyd^{2-} **1**; L = $dicyd^{2-}$ **2**; L = Cl_2dicyd^{2-} **3**; L = Cl_4dicyd^{2-} **4**.

Table 1. Cyclic Voltammetry Data[a] of [{Ru(ttpy)(bpy)}$_2$(μ-L)]$^{2+}$ Complexes, [Ru(ttp)(bpy)Cl]$^+$ and [AsPh$_4$]$_2$dicyd

compound	L(−1/−2)	L(0/−1)	Ru(III/II)
1	0.23 (71)[c]	0.72 (71)[d]	
2	0.33 (83)[c]	0.80 (73)[d]	
3	0.54 (66)[c]	0.96 (106)[d]	
4	0.66 (66)[c]	1.03 (110)[d]	
[Ru(ttpy)(bpy)Cl]$^+$			1.02 (85)
[AsPh$_4$]$_2$dicyd	−0.20[b]	0.47[b]	

[a]Data in volts vs NHE, 0.1 M TBAH in DMF, scan rate 100 mV/s, anodic and cathodic peak. [b]In acetonitrile, reference 9. [c]Assignment supported by EPR studies. [d]Assignment supported by semiempirical calculations.

dx.doi.org/10.1021/ic401316g | Inorg. Chem. 2013, 52, 11060−11066

processes. These couples shift to more positive potentials as electron-withdrawing substituents are added to the dicyd^{2-} ligand.

EPR spectroscopy of the dinuclear complexes establishes the first oxidation couple, $[\{Ru(ttpy)(bpy)\}_2(\mu\text{-L})]^{3+/2+}$, as ligand centered L(−1/−2) while the second oxidation couple is formally assigned to a L(0/−1) couple based on semiempirical calculations as discussed below.

Figure 2 shows the broad low-temperature EPR spectrum of the mononuclear complex $[Ru(trpy)(bpy)(2,4\text{-}Cl_2pcyd)]^{2+}$ that

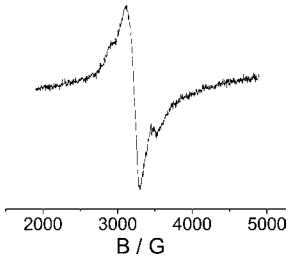

Figure 2. EPR spectrum of oxidized mononuclear $[Ru(trpy)(bpy)(2,4\text{-}Cl_2pcyd)][PF_6]$ in DMF at 110 K.

is typical of a low spin d^5 Ru(III) ion.[16] The g components are g_1 = 2.34, g_2 = 2.10, and g_3 = 1.92, and the average g value g_{av} = 2.13. Oxidation of the dinuclear complex $[\{Ru(ttpy)(bpy)\}_2(\mu\text{-dicyd})]^{2+}$ (**2**) in DMF solution gave the EPR spectra shown in Figure 3. In contrast to $[Ru(trpy)(bpy)(2,4\text{-}Cl_2pcyd)]^{2+}$, $\mathbf{2}^+$

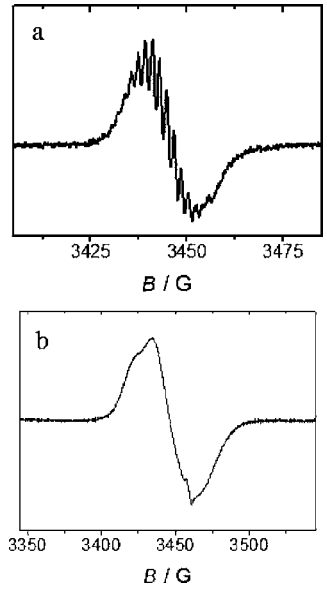

Figure 3. EPR spectra of $[\{Ru(ttpy)(bpy)\}_2(\mu\text{-dicyd})]^{3+}$ $\mathbf{2}^+$ in DMF solution at (a) room temperature and (b) at 110 K (a weak signal from an organic impurity is observed at g = 2.003).

gave a room temperature isotropic spectrum (Figure 3a) at g = 2.009 which is relatively narrow and exhibits several hyperfine lines split by approximately 1.7 G. Although the partial resolution did not allow us to fully analyze the hyperfine coupling pattern, the splitting is similar to the EPR spectrum of the potassium salt of the dicyd anion radical with g = 2.0023 and hyperfine splitting varying between 1 and 5 G.[17] These results strongly support an oxidized (radical) bridging ligand in $\mathbf{2}^+$. As shown in Figure 3b, a lowering of the temperature to 110 K (frozen solution) results in the loss of hyperfine information but reveals a small g anisotropy (g_1, g_2, g_3 = 2.025, 2.011, and 2.00, respectively). The calculated g_{av} = 2.012 close to the free electron value of 2.0023 and the $\Delta g = g_1 - g_3$ = 0.025 indicate little mixing of ruthenium ions with their high spin−orbit coupling contributions in the ligand-localized SOMO.[18] Similar results have been reported for the complex $[\{Ru(tpy)(thd)\}_2(\mu\text{-dicyd})]^+$, where thd$^-$ is 2,2,6,6-tetramethyl-3,5-heptanedione.[5]

Chloro substitution on dicyd^{n-} should induce greater mixing of metal and ligand orbitals upon oxidation of the complex. This is illustrated by the EPR spectrum of $\mathbf{4}^+$ at 110 K (Figure 4; no room temperature signal) which exhibits greater g

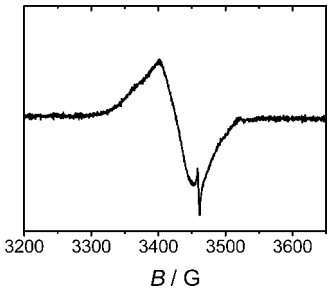

Figure 4. EPR spectrum of $[\{Ru(ttpy)(bpy)\}_2(\mu\text{-}Cl_4dicyd)]^{3+}$ $\mathbf{4}^+$ in DMF solution at 110 K. A weak signal from an organic impurity is observed at g = 2.003.

anisotropy at g_1, g_2, g_3 = 2.06, 2.03, and about 2.02, respectively, and a larger g_{av} = 2.037 and Δg = 0.04. These values are still consistent with a dominant contribution to the SOMO by the bridging ligand and so the formal assignment for all $[\{Ru(ttpy)(bpy)\}_2(\mu\text{-L})]^{3+/2+}$ couples is suggested to be a $L^{\bullet-}/L^{2-}$ reduction couple.

EPR spectroscopy is the method of choice for evaluating the noninnocence of metal complexes containing redox-active ligands and indeed, in this study, EPR has shown that $[Ru(trpy)(bpy)(2,4\text{-}Cl_2pcyd)]^{2+}$ is a Ru(III) species with metal centered spin while $\mathbf{1}^+$−$\mathbf{4}^+$ are radical complexes with ligand centered spin. However, cost and availability of EPR instrumentation to researchers are significant disadvantages, and some radical complexes can be EPR silent even at very low temperatures. In these cases, paramagnetic ^{1}H NMR spectroscopy may provide evidence of SOMO parentage. With this in mind, the oxidized complexes $\mathbf{1}^+$−$\mathbf{4}^+$ were prepared by reacting **1**−**4** with NO^+ BF_4^- in acetonitrile solution, checking for completeness by comparison to the spectra of $\mathbf{1}^+$-$\mathbf{4}^+$ as obtained by spectroelectrochemical methods (vide infra). Evaporation of acetonitrile left the crude oxidized complexes which were used without further purification to investigate their paramagnetic ^{1}H NMR spectroscopy. The spectra of $\mathbf{1}^+$−$\mathbf{4}^+$ showed broad, poorly resolved signals with aromatic chemical shifts belonging to ttpy between 6 and 15 ppm that could not be assigned unambiguously. However, the chemical shift of the *t*-butyl group for a given complex could be readily identified because it was largely unaffected by oxidation, being shifted downfield by about 0.02 ppm relative to its diamagnetic chemical shift range from 1.39 to 1.40 ppm (in the complexes of this study). The situation is quite different for the complex $[Ru(ttpy)(bpy)Cl]^{2+}$ which was prepared in the same manner as that for $\mathbf{1}^+$−$\mathbf{4}^+$. For this complex, the chemical shift of the *t*-butyl group was shifted *upfield* to 1.09 ppm from its diamagnetic chemical shift of 1.42

dx.doi.org/10.1021/ic401316g | *Inorg. Chem.* 2013, 52, 11060−11066

ppm. Assuming that pseudocontact shift contribution to the isotropic shift is small,[19] the contact shift must result from spin density being placed on the *t*-butyl hydrogens through a combination of σ and π spin polarization of ttpy from spin density originating on Ru(III).

Electronic and IR spectroelectrochemistry were performed on the $[\{Ru(ttpy)(bpy)\}_2(\mu\text{-}L)]^{2+}$ complexes to gain a greater understanding of these complexes with non-innocent ligands and, more specifically, to see if the introduction of more metal character to the SOMO of $[\{Ru(ttpy)(bpy)\}_2(\mu\text{-}L)]^{3+}$ results in significantly perturbed electronic and IR spectra. The spectroelectrochemical studies of the complexes of this study showed reversible processes with at least 95% recovery of the initial spectrum except where otherwise noted. Electronic absorption data has been compiled in Table 2.

Table 2. Quantitative Electronic Absorption Data of $[\{Ru(ttpy)(bpy)\}_2(\mu\text{-}L)]^{2+/3+/4+}$ Complexes in DMF, 0.1 M TBAH

complex	wavelength in nm (molar absorption coefficient M^{-1} cm^{-1})
1	364 (sh,29300), 498 (21000)
$\mathbf{1}^{+}$	399 (sh,23900), 491 (22300), 1023 (13300)
$\mathbf{1}^{2+}$	463 (24200), 918(17100)
2	364 (sh,30600), 493(23400)
$\mathbf{2}^{+}$	383 (sh,27800), 487 (25000), 1083(17700)
$\mathbf{2}^{2+}$	457 (26700), 959 (27500)
3	364 (sh,29800), 482 (22800)
$\mathbf{3}^{+}$	358 (sh,30300), 426 (30000), 482(27000), 1265(18800)
$\mathbf{3}^{2+}$	482(27000), 855 (9900)
4	364 (sh, 38100), 485 (22200)
$\mathbf{4}^{+}$	430 (37000), 489 (sh,26300), 1376 (25200)
$\mathbf{4}^{2+}$	489 (26000), 869 (8500), 1376 (6300)

Figure 5 shows the spectroelectrochemical oxidation of **2** to the singly oxidized $\mathbf{2}^{+}$ and doubly oxidized $\mathbf{2}^{2+}$ complexes. These results are similar to those of complex **1**, which have been placed in Supporting Information, Figure S9. In Figure 5a, oxidation of the bridging ligand results in the appearance of a strong NIR absorption with λ_{max} = 1083 nm. Because EPR spectroscopy supports a [Ru(II), $L^{\bullet-}$, Ru(II)] oxidation state description, the band could be assigned to Ru(II) dπ to dicyd pπ, metal-to-ligand charge transfer (MLCT) transition or a dicyd ligand centered transition. DFT calculations were attempted to settle this issue; however, the calculations would not converge.[20] Semiempirical calculations show a HOMO that is mostly ligand centered in agreement with EPR studies and possible low energy transitions from filled pπ MOs of the $dicyd^{\bullet-}$ ligand thereby supporting a mostly ligand centered transition (Supporting Information, Figure S10). In Figure 5b, further oxidation increases the intensity and slightly shifts this band to higher energies with λ_{max} = 959 nm. Semiempirical calculations of $\mathbf{2}^{2+}$ assuming a singlet ground state show mostly ligand centered HOMO and LUMO (Supporting Information, Figure S11) which arises from the oxidation of the radical bridging ligand to $dicyd^0$. *N,N′*-Dicyanoquinonediimine ($dicyd^0$ or DCNQI in the literature) and its substituted derivatives have been isolated as diamagnetic yellow compounds with no NIR absorption.[21] The band with λ_{max} = 959 nm is therefore not easily explained by a ligand centered transition, and it is suggested that, if $\mathbf{2}^{2+}$ can be formally represented by [Ru(II), L^0, Ru(II)]$^{4+}$, this band is a mostly Ru(II) to L^0 MLCT transition.

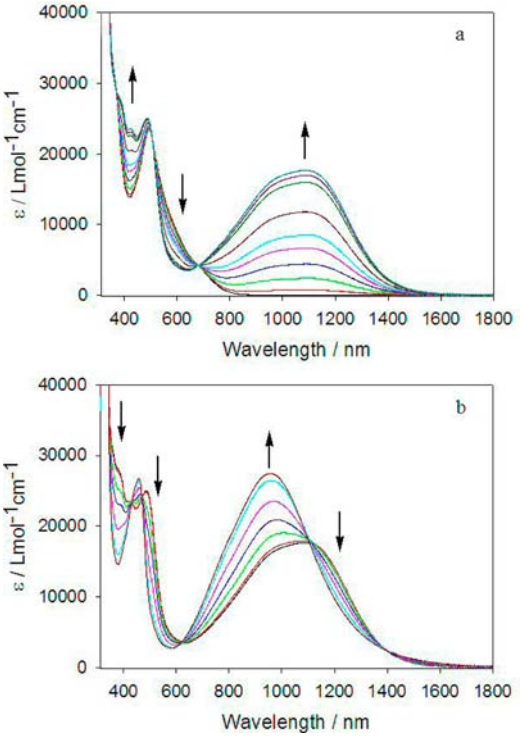

Figure 5. Visible/NIR spectroelectrochemical oxidation of $[\{Ru(ttpy)(bpy)\}_2(\mu\text{-dicyd})]^{2+}$ **2** to form (a) $[\{Ru(ttpy)(bpy)\}_2(\mu\text{-dicyd})]^{3+}$ $\mathbf{2}^{+}$ and (b) $[\{Ru(ttpy)(bpy)\}_2(\mu\text{-dicyd})]^{4+}$ $\mathbf{2}^{2+}$; in DMF, 0.1 M TBAH.

Figure 6 shows the visible/NIR spectroelectrochemical oxidation of **3** to the $\mathbf{3}^{+}$ and $\mathbf{3}^{2+}$ complexes. For **4**, the first and second oxidations gave similar spectral changes to those shown in Figure 5 except that the second oxidation was incomplete because of poor reversibility. The data have been placed in Supporting Information, Figure S12. Similar to Figure 5a, in Figure 6a, an intense NIR absorption band appears at λ_{max} = 1265 nm with the formation of $\mathbf{3}^{+}$ which we again assign to a ligand centered transition. However, the second oxidation (Figure 6b) results in a relatively large shift of the band to shorter wavelengths with λ_{max} = 855 nm, a significant decrease in the intensity of this band, and the appearance of a low energy absorption (1200−1800 nm). This is very different from the spectral changes associated with the formation of $\mathbf{2}^{2+}$ in Figure 5b and may result from a significant contribution from [Ru(III), $L^{\bullet-}$, Ru(II)]$^{4+}$ to $\mathbf{3}^{2+}$.

Further evidence for the participation of ruthenium in the $\mathbf{3}^{+}$ complex's SOMO can be found in IR spectroelectrochemical studies.

Figure 7 shows spectral changes that occur in the cyanamide stretching region with the formation of $[Ru(trpy)(bpy)(2,4\text{-}Cl_2pcyd)]^{2+}$ from the monocation in DMF. Upon oxidation to Ru(III) there occurs a loss of the band at 2170 cm^{-1} and the appearance of two weak bands centered at 2040 and 2270 cm^{-1}. The band at 2270 cm^{-1} is associated with decomposition of the complex, and indeed only 85% reversibility to the original dication spectrum was observed. The weak band at 2040 cm^{-1} is expected from IR studies of $[Ru(NH_3)_5(pcyd)]^{2+}$ and $[Ru(NH_3)_3(bpy)(pcyd)]^{2+}$ where pcyd is a phenylcyanamido ligand.[22] These studies showed that oxidation of Ru(II) to Ru(III) shifts ν(NCN) to lower frequencies because of a shift of cyanamide resonance forms as shown below

dx.doi.org/10.1021/ic401316g | *Inorg. Chem.* 2013, 52, 11060−11066

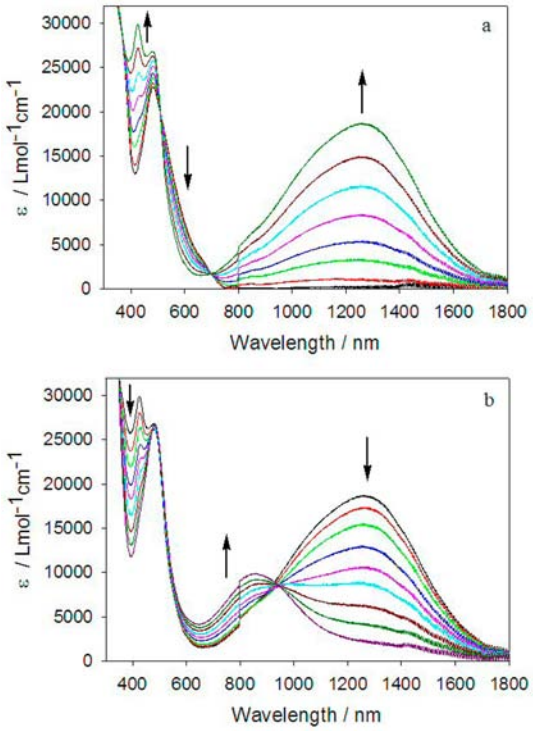

Figure 6. Visible NIR spectroelectrochemical oxidation of $[\{Ru(ttpy)(bpy)\}_2(\mu\text{-}Cl_2dicyd)]^{2+}$ **3** to form a) $[\{Ru(ttpy)(bpy)\}_2(\mu\text{-}Cl_2dicyd)]^{3+}$ $\mathbf{3}^{+}$ and b) $[\{Ru(ttpy)(bpy)\}_2(\mu\text{-}Cl_2dicyd)]^{4+}$ $\mathbf{3}^{2+}$, in DMF, 0.1 M TBAH.

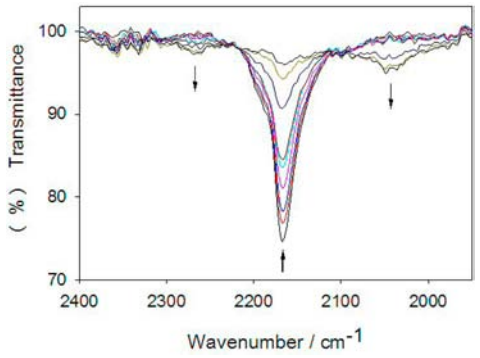

Figure 7. IR spectral changes associated with the oxidation of $[Ru(trpy)(bpy)(2,4\text{-}Cl_2pcyd)](PF_6)$ in DMF, 0.1 M TBAH. Only 85% recovery of initial spectrum.

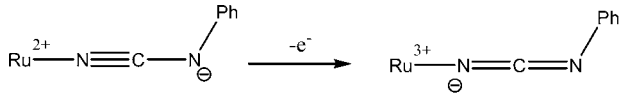

IR spectroelectrochemistry showing the oxidation of the free dianion ligand Me_2dicyd^{2-} in DMF has been placed in Supporting Information, Figure S11. A DMF solution of Me_2dicyd^{2-} shows a strong ν(NCN) band at 2070 cm^{-1} and a far weaker band at 2110 cm^{-1}. Cyanamide groups can adopt *syn*- and *anti*-conformations and so a multiplicity of ν(NCN) bands is not unexpected. Upon oxidation to the anion radical Supporting Information, Figure S13a, the intensity of the band at 2070 cm^{-1} drops and new bands appear at 2120 and 2090 cm^{-1}. Oxidation to Me_2dicyd^{0} (Supporting Information, Figure S13b) sees a further decrease in intensity and new bands appearing at 2170 and 2220 cm^{-1}. Overall, oxidation of Me_2dicyd^{2-} results in a decrease in intensity and a shift of ν(NCN) to higher frequencies.

Figure 8 shows the IR spectral changes that occur upon oxidation of oxidation of **2** to the $\mathbf{2}^{+}$ and $\mathbf{2}^{2+}$ cations in DMF

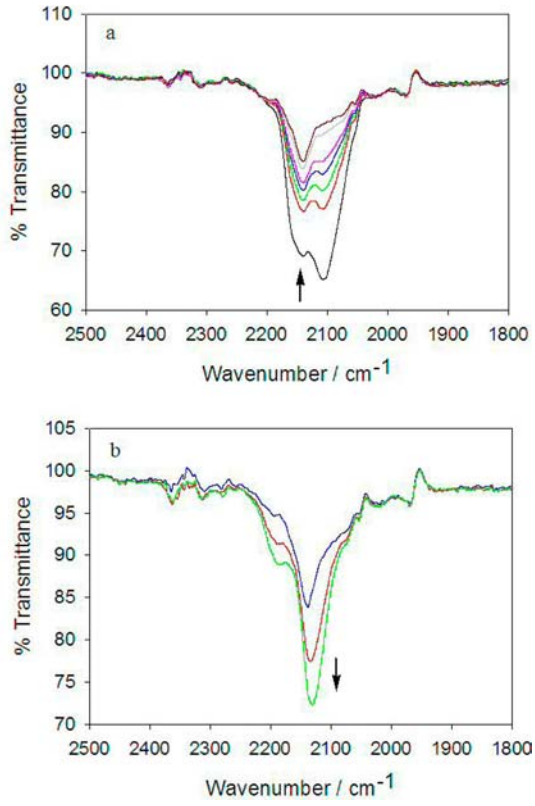

Figure 8. IR spectroelectrochemical oxidation of $[\{Ru(ttpy)(bpy)\}_2(\mu\text{-}dicyd)]^{2+}$ **2** to form (a) $[\{Ru(ttpy)(bpy)\}_2(\mu\text{-}dicyd)]^{3+}$ $\mathbf{2}^{+}$ and (b) $[\{Ru(ttpy)(bpy)\}_2(\mu\text{-}dicyd)]^{4+}$ $\mathbf{2}^{2+}$, in DMF, 0.1 M TBAH.

solution. In Figure 8a and similar to Me_2dicyd (Supporting Information, Figure S13a), the initial spectrum shows at least two overlapping ν(NCN) bands which are probably due to a mixture of *syn*- and *anti*-conformations in solution. Crystal structures of dinuclear ruthenium complexes bridged by dicyd ligands have shown both *syn* and *anti*-conformations, but the most common structure is that of a planar *anti*-conformation.[5,8,13,23] Upon oxidation to 2^{+}, the intensity of the ν(NCN) bands decreases with only a slight shift to higher frequencies. Based on the EPR data, the single cyanamide stretching frequency must be a consequence of a SOMO possessing equivalent contributions from the cyanamide groups of the bridging ligand. Further oxidation to $\mathbf{2}^{2+}$ (Figure 8b), slightly shifts the ν(NCN) band to lower energy and increases its intensity. The IR spectroelectrochemical oxidations of **1** and **3** are very similar to these results and have been placed in Supporting Information, Figures S14 and S15. Oxidation of **4** shows significantly different behavior.

In Figure 9, the oxidation of **4** to $\mathbf{4}^{+}$ in DMF causes a decrease in intensity of the ν(NCN) band at 2150 cm^{-1} and the growth of a new band at 2100 cm^{-1}. This shift to lower frequencies is very different from that of $\mathbf{2}^{+}$ in Figure 8a, and it is suggested to be due to a greater contribution of ruthenium character to the SOMO. A single band ν(NCN) at 2100 cm^{-1} in Figure 8 is consistent with a delocalized state, and indeed 2100 cm^{-1} is the average of Ru(II) and Ru(III) cyanamide

dx.doi.org/10.1021/ic401316g | *Inorg. Chem.* 2013, 52, 11060−11066

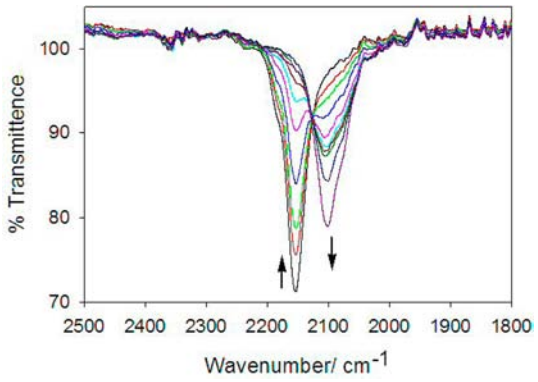

Figure 9. IR spectroelectrochemical oxidation of $[\{Ru(ttpy)(bpy)\}_2(\mu\text{-}Cl_4dicyd)]^{2+}$ **4** to form $[\{Ru(ttpy)(bpy)\}_2(\mu\text{-}Cl_4dicyd)]^{3+}$ $\mathbf{4}^+$ in DMF, 0.1 M TBAH.

stretching frequencies from Figure 7. However, as already discussed, the EPR data do not support a ruthenium-centered SOMO and indicate the caution which must be invoked before making state assignments based on IR data alone.

CONCLUSIONS

EPR spectra of the $[\{Ru(ttpy)(bpy)\}_2(\mu\text{-}L)]^{3+}$ ions show predominately organic radical features, confirming ligand centered spins and thus the complexes' oxidation states are best formulated as [Ru(II), $L^{\bullet-}$, Ru(II)]. Visible/NIR and IR spectra of $[\{Ru(ttpy)(bpy)\}_2(\mu\text{-}L)]^{3+,4+}$ ions were obtained by spectroelectrochemical methods. For the $[\{Ru(ttpy)(bpy)\}_2(\mu\text{-}L)]^{3+}$ complexes, spectral variations were rationalized in terms of the nature of the substituted bridging ligand L and variable ruthenium d-orbital contributions to the mostly ligand-centered SOMO.

ASSOCIATED CONTENT

Supporting Information

^{1}H NMR spectra, COESY, and Table of chemical shifts of all the complexes (eight figures and a table), Vis-NIR and IR spectroelectrochemical spectra (four figures) and two figures showing the orbital energies and frontier molecular orbitals of $\mathbf{2}^+$ and $\mathbf{2}^{2+}$. This material is available free of charge via the Internet at http://pubs.acs.org.

AUTHOR INFORMATION

Corresponding Author

*E-mail: robert_crutchley@carleton.ca.

Notes

The authors declare no competing financial interest.

ACKNOWLEDGMENTS

This work is supported by Carleton University and the Natural Sciences and Engineering Research Council of Canada.

REFERENCES

(1) (a) Kaim, W.; Schwederski, B. *Coord. Chem. Rev.* **2010**, *254*, 1580. (b) Lyons, C. T.; Stack, T. D. P. *Coord. Chem. Rev.* **2012**, *257*, 528.
(2) (a) Boyer, J. L.; Rochford, J.; Tsai, W.-T.; Muckerman, J. T.; Fujita, E. *Coord. Chem. Rev.* **2010**, *254*, 309. (b) Lyaskovskyy, V.; de Bruin, B. *ACS Catal.* **2012**, *2*, 270.
(3) Marder, S. R.; Kippelen, B.; Jen, A. K.-Y.; Peyghambarian, N. *Nature* **1997**, *388*, 845.
(4) (a) Low, P. J. *Coord. Chem. Rev.* **2013**, *257*, 1507. (b) Das, A. K.; Sarkar, B.; Fiedler, J.; Zalis, S.; Hartenbach, I.; Strobel, S.; Lahiri, G. K.; Kaim, W. *J. Am. Chem. Soc.* **2009**, *131*, 8895. (c) Chakraborty, S.; Laye, R. H.; Paul, R. L.; Gonnade, R. G.; Puranik, V. G.; Ward, M. D.; Lahiri, G. K. *J. Chem. Soc., Dalton Trans.* **2002**, 1172. (d) Ward, M. D.; McCleverty, J. A. *J. Chem. Soc., Dalton Trans.* **2002**, 275.
(5) Naklicki, M. L.; Gorelsky, S. I.; Kaim, W.; Sarkar, B.; Crutchley, R. J. *Inorg. Chem.* **2012**, *51*, 1400.
(6) Fabre, M.; Jaud, J.; Hliwa, M.; Launay, J.-P.; Bonvoisin, J. *Inorg. Chem.* **2006**, *45*, 9332.
(7) Rezvani, A. R.; Evans, C. E. B.; Crutchley, R. J. *Inorg. Chem.* **1995**, *34*, 4600.
(8) Mosher, P. J.; Yap, G. P. A.; Crutchley, R. J. *Inorg. Chem.* **2001**, *40*, 550.
(9) Aquino, M. A. S.; Lee, F. L.; Gabe, E. J.; Bensimon, C.; Greedan, J. E.; Crutchley, R. J. *J. Am. Chem. Soc.* **1992**, *114*, 5130.
(10) Crutchley, R. J. *Coord. Chem. Rev.* **2001**, *219*−*221*, 125.
(11) Constable, E. C.; Harverson, P.; Smlth, D. F.; Whall, L. A. *Tetrahedron* **1994**, *50*, 7799.
(12) Gennett, T.; Milner, D. F.; Weaver, M. J. *J. Phys. Chem.* **1985**, *89*, 2787.
(13) Evans, C. E. B.; Yap, G. P. A.; Crutchley, R. J. *Inorg. Chem.* **1998**, *37*, 6161.
(14) (a) Al-Noaimi, M.; Yap, G. P. A.; Crutchley, R. J. *Inorg. Chem.* **2004**, *43*, 1770. (b) Evans, C. E. B.; Ph.D. Thesis, Carleton University, Ottawa, Canada, 1997.
(15) Krejcik, M.; Danek, M.; Hartl, F. *J. Electroanal. Chem.* **1991**, *317*, 179.
(16) (a) Patra, S.; Sarkar, B.; Mobin, S. M.; Kaim, W.; Lahiri, G. K. *Inorg. Chem.* **2003**, *42*, 6469. (b) Poppe, J.; Moscherosch, M.; Kaim, W. *Inorg. Chem.* **1993**, *32*, 2640.
(17) Gerson, F.; Gescheidt, G.; Möcke1, R.; Aumüller, A.; Erk, P.; Hünig, S. *Helv. Chim. Acta* **1988**, *71*, 1665.
(18) Kasack, V.; Kaim, W.; Binder, J.; Jordanov, J.; Roth, E. *Inorg. Chem.* **1995**, *34*, 1924.
(19) Distance from Ru(III) to the *t*-butyl group is about 10.5 Å and pseudocontact shift is proportional to $1/r^3$.
(20) Serge Gorelsky, personal communication, April 4, 2013. Time-dependent DFT calculations at the B3LYP/DZVP level of theory failed to converge.
(21) (a) Aumüller, A.; Hünig, S. *Justus Liebigs Ann. Chem.* **1986**, 142. (b) Hünig, H.; Bau, R.; Kemmer, M.; Meixner, H.; Metzenthin, T.; Peter, K.; Sinzger, K.; Gulbis, J. *Eur. J. Org. Chem.* **1998**, 335.
(22) DeRosa, M. C.; White, C. A.; Evans, C. E. B.; Crutchley, R. J. *J. Am. Chem. Soc.* **2001**, *123*, 1396.
(23) Rezvani, A. R.; Bensimon, C.; Cromp, B.; Reber, C.; Greedan, J. E.; Kondratiev, V. V.; Crutchley, R. J. *Inorg. Chem.* **1997**, *36*, 3322.